Published in final edited form as:

Mol Psychiatry. 2018 June ; 23(6): 1453–1465. doi:10.1038/mp.2016.260.

Neurons derived from patients with bipolar disorder divide into intrinsically different sub-populations of neurons, predicting the patients' responsiveness to lithium

S Stern[1,7], **R Santos**[1,2,7], **MC Marchetto**[1], **APD Mendes**[1], **GA Rouleau**[3], **S Biesmans**[4], **Q-W Wang**[5], **J Yao**[5], **P Charnay**[2], **AG Bang**[4], **M Alda**[6], and **FH Gage**[1]

[1]Laboratory of Genetics, The Salk Institute for Biological Studies, La Jolla, CA, USA

[2]Ecole Normale Supérieure, PSL Research University, CNRS, Inserm, Institut de Biologie de l'Ecole Normale Supérieure (IBENS), Paris, France

[3]Montreal Neurological Institute, Department of Neurology and Neurosurgery, McGill University, Montreal, QC, Canada

[4]Conrad Prebys Center for Chemical Genomics, Sanford Burnham Prebys Medical Discovery Institute, La Jolla, CA, USA

[5]State Key Laboratory of Membrane Biology, Tsinghua-Peking Joint Center for Life Sciences, School of Life Sciences, IDG/McGovern Institute for Brain Research, Tsinghua University, Beijing, China

[6]Department of Psychiatry, Dalhousie University, Halifax, NS, Canada. Correspondence: Professor FH Gage, Laboratory of Genetics, The Salk Institute for Biological Studies, The Salk Institute, 10010 North Torrey Pines Road, La Jolla, CA 92037, USA

Abstract

Bipolar disorder (BD) is a progressive psychiatric disorder with more than 3% prevalence worldwide. Affected individuals experience recurrent episodes of depression and mania, disrupting normal life and increasing the risk of suicide greatly. The complexity and genetic heterogeneity of psychiatric disorders have challenged the development of animal and cellular models. We recently reported that hippocampal dentate gyrus (DG) neurons differentiated from induced pluripotent stem cell (iPSC)-derived fibroblasts of BD patients are electrophysiologically hyperexcitable. Here we used iPSCs derived from Epstein–Barr virus-immortalized B-lymphocytes to verify that the hyperexcitability of DG-like neurons is reproduced in this different cohort of patients and cells. Lymphocytes are readily available for research with a large number of banked lines with associated patient clinical description. We used whole-cell patch-clamp recordings of over 460 neurons to characterize neurons derived from control individuals and BD patients. Extensive functional analysis showed that intrinsic cell parameters are very different between the two groups

Correspondence to: FH Gage.

[7]These authors contributed equally to this work.

CONFLICT OF INTEREST

The authors declare no conflict of interest.

Supplementary Information accompanies the paper on the Molecular Psychiatry website (http://www.nature.com/mp)

of BD neurons, those derived from lithium (Li)-responsive (LR) patients and those derived from Li-non-responsive (NR) patients, which led us to partition our BD neurons into two sub-populations of cells and suggested two different subdisorders. Training a Naïve Bayes classifier with the electrophysiological features of patients whose responses to Li are known allows for accurate classification with more than 92% success rate for a new patient whose response to Li is unknown. Despite their very different functional profiles, both populations of neurons share a large, fast after-hyperpolarization (AHP). We therefore suggest that the large, fast AHP is a key feature of BD and a main contributor to the fast, sustained spiking abilities of BD neurons. Confirming our previous report with fibroblast-derived DG neurons, chronic Li treatment reduced the hyperexcitability in the lymphoblast-derived LR group but not in the NR group, strengthening the validity and utility of this new human cellular model of BD.

INTRODUCTION

Bipolar disorder (BD) affects more than 3% of the worldwide population.[1–3] People with BD experience episodes of mania and depression that often repeat periodically.[4,5] About 50% of BD patients suffer from hallucinations or delusions.[6,7] Left untreated, patients are at a high risk of suicide.[8,9] The main current treatment for BD is chronic lithium (Li) therapy.[10,11] Li is known to act through an inhibition of glycogen synthase kinase-3β,[12] modulation of the neurotransmitters and signals impacting the cytoskeleton,[13] an increase in neurotrophic molecules, changes in the metabolic enzymes and signaling pathways involved in the antioxidant response, apoptosis and endoplasmic reticulum stress.[14–16] However, the exact mechanism of how Li stabilizes mood is not completely understood. Only ~ 30% of BD patients respond fully to Li (LR);[17,18] in this study, half of our patients were Li-non-responders (NR).

BD is a highly heritable disorder, with a risk ratio of 8–10[19] for first-degree relatives and heritability of ~ 85% derived from twin studies.[20,21] The genetics of BD is not well known but it is considered to be polygenic, sharing common polygenic variations with schizophrenia.[22] Genome-wide association studies (GWAS) reveal several genetic variants, including CACNA1C, ODZ4, ANK3 and NCAN,[23–25] and several associated single-nucleotide polymorphisms along with multiple gene factors.[26,27] Owing to the complexity and heterogeneity of the genetics of BD, it is difficult to develop gene-targeted or phenotypic animal models,[28,29] which has resulted in slow advances in our understanding of the disease, especially at the cellular level.

The reported neuropathology of BD includes reductions in neuronal and glial density in the prefrontal cortex, anterior cingulate cortex and hippocampus,[30–33] although other studies of the anterior cingulate cortex have found no difference in neuronal and glial density.[34] Genes and pathways associated with neurotransmitters have been shown to be altered in BD patients,[35] along with changes in the levels of several neuromodulators and neurotransmitters.[36,37] Alterations in the excitatory/inhibitory ratio have also been demonstrated,[38,39] and mitochondrial cytopathies and dysfunction have been associated with BD.[40,41]

The introduction of induced pluripotent stem cell (iPSC) technology has greatly enabled the advancement of research of psychiatric disorders, making the modeling of human disease possible. Using patch-clamp recordings and somatic calcium imaging, we reported recently[42] that hippocampal dentate gyrus (DG) granule-cell-like neurons that were differentiated from fibroblast-derived iPSCs were hyperexcitable. The results were significant but the size and representativeness of the patient cohort were limited.[43] We therefore undertook the task of replicating this observation in a separate cohort of patients and using a different somatic cell type to generate iPSCs. Our results demonstrate that immortalized B-lymphocytes[44,45] can be reprogrammed to iPSCs and then can be induced to DG-like neurons; the DG granule-cell hippocampal neurons differentiated from BD patients in this new cohort are hyperexcitable. We further show that BD neurons can be divided into two subgroups, each with very distinct and different electrophysiological features depending on their responsiveness to Li. Training a Naïve Bayes (NB) classifier on the electrophysiological features of known patients can successfully predict the responsiveness of an unknown patient to Li. The electrophysiological feature that is shared by the neurons from the two subgroups of BD patients is a large, fast after-hyperpolarization (AHP), which we suggest is a key to the BD neurons' fast spiking abilities.

MATERIALS AND METHODS

Patient selection and clinical assessment

Probands with BD were recruited from our ongoing genetic studies.[46] The control subjects were either healthy volunteers or married-in relatives of our probands. All study participants underwent diagnostic assessments that followed a strict procedure: after signing an informed consent they were interviewed by pairs of experienced clinician researchers blind to the subject status. The interviews were followed by consensus diagnosis (according to Research Diagnostic Criteria[47] and DSM-IV) established by a second blind panel of expert clinical researchers. As the primary diagnostic tool, we used the Schedule for Affective Disorders and Schizophrenia— Lifetime version.[48] All interviewers had undergone extensive training previously and established very good inter-rater reliability for both diagnostic[49] and treatment response evaluations.[50]

Patients with BD treated with Li for a minimum of 1 year were evaluated for their treatment response. We used all available information, including data from clinical records, diagnostic interviews and prospective follow-up, and converted it to a score on a 0–10 scale previously validated and adopted by a number of research groups.[50–52] A score of 7 or higher indicates positive response to treatment.[51,52] Basic demographic and clinical data appear in Supplementary Table 1.

Reprogramming and pluripotency analysis

Epstein–Barr virus (EBV)-immortalized B-lymphocytes were reprogrammed using the Yamanaka Episomal vector set described by Okita *et al.*,[53] consisting of three sets of episomal plasmids expressing reprograming factors: pCXLE-hOCT3/4-shp53, pCXLE-hSK (SOX2, KLF4) and pCXLE-hUL (L-MYC, LIN28). We reprogrammed lymphocytes from a total of six patients with BD: three were responders (SBP005, SBP007, SBP010) and three

were non-responders (SBP001, SBP002, SBP004) to LiCl treatment. We also reprogrammed lymphocytes from four age- and gender-matched neurotypical individuals as controls (SBP008, SBP009, SBP011, SBP012). After reprogramming, at least three iPSC colonies were selected for further characterization. Quality control criteria for validation of iPSC lines included (a) absence of integration of episomal reprograming plasmids, presence of normal karyotype; (b) positive staining for four pluripotent markers (Sox2, Oct4, Nanog and Tra-1-81) and (c) authentication of cell lines using a comparison of a 16-loci short tandem repeat profile between the iPSC clones and the original lymphoblast line (performed by Genetica DNA Lab, Cincinnati, OH, USA). The episomal vector copy number per cell was determined by the quantitative PCR method. The *Foxb15* gene served as a chromosome number control to determine the cell number input. The primer sets for Oct4, Klf4 and L-Myc were used to determine the copy number of three vectors. The standard curve for each quantitative PCR assay was performed using the plasmid DNA that contained the target sequence. The primer sequence and PCR condition were described in Okita *et al.*[53]

Immunofluorescence assays

The antibodies used for pluripotency and neuronal characterization were anti-hOct4 (Cell Signaling, Danvers, MA, USA; cat. no. 2840S), anti-hSox2 (Cell Signaling; cat. no. 3579S), anti-hNanog antibody (Cell Signaling; cat. no. 4903S), Tra-1-81 (Cell Signaling; cat. no. 4745S), anti-MAP2 (Abcam; cat. no. 5392) and anti-GFP (Abcam, San Francisco, CA, USA; cat. no. 6673).

Electrophysiology

Neurons were infected with the Prox1::eGFP lentiviral vector at 8 days differentiation. Neurons on glass coverslips were transferred to a recording chamber in a standard recording medium containing (in mM): 10 HEPES, 4 KCl, 2 $CaCl_2$,1 $MgCl_2$, 139 NaCl, 10 D-glucose (310 mOsm, pH 7.4). Whole-cell patch-clamp recordings were performed from Prox1::eGFP highlighted DG-like neurons (the neurons patched were typically the larger cells, with the bright Prox1::eGFP expression), usually after 20–30 days of differentiation and in a range of 10–45 days of differentiation. Patch electrodes were filled with internal solutions containing (in mM): 130 K-gluconate, 6 KCl, 4 NaCl, 10 Na-HEPES, 0.2 K-EGTA, 0.3 GTP, 2 Mg-ATP, 0.2 cAMP, 10 D-glucose, 0.15% biocytin and 0.06% rhodamine. The pH and osmolarity of the internal solution were brought close to physiological conditions (pH 7.3, 290–300 mOsm) (pipette tip resistance was typically 10–15 MΩ). Signals were amplified with a Multiclamp700B amplifier (Sunnyvale, CA, USA) and recorded with Clampex 10.2 software (Axon Instruments, Union City, CA, USA). Data were acquired at a sampling rate of 20 kHz and analyzed using Clampfit-10 and the software package MATLAB (release 2014b; The MathWorks, Natick, MA, USA). All measurements were conducted at room temperature.

Li treatment

Cultures were treated chronically with 1 mM LiCl starting at 14 days differentiation. Every second day, 50% of the differentiation medium containing 1 mM LiCl was exchanged. Electrophysiological recordings were conducted at 22–30 days differentiation.

Electrophysiology analysis

Total evoked action potentials—Cells were typically held in current clamp mode near −60 mV with a steady holding current, and current injections were given starting 12 pA below the steady holding current, in 3-pA steps 400 ms in duration. A total of 35 depolarization steps were given. Neurons that needed more than 50 pA to be held at −60 mV were discarded from the analysis. The total number of action potentials was counted in the 35 depolarization steps, starting from the first depolarization step, which is 12 pA below the current that causes the membrane potential to be at −60 mV (this current is usually 0, unless there is some leakage current), with the last step being in a current injection of 90 pA.

For the most excitable data set, we used 35 action potentials as the threshold between 'hyper' and 'hypo' neurons. This threshold was chosen as approximately the total number of evoked action potentials in the control neurons+one half of the standard deviation.

Action potential shape analysis—The first evoked action potential was used for spike shape analysis (with the lowest injected current needed for eliciting an action potential). Spike threshold was the membrane potential at which the slope of the depolarizing membrane potential increased markedly, resulting in an action potential (the first maximum in the second derivative of the voltage vs time). The 5-ms AHP amplitude was calculated as the difference between the threshold for spiking and the value of the membrane potential 5 ms after the potential returned to cross the threshold value at the end of the action potential. The spike amplitude was calculated as the difference between the maximum membrane potential during a spike and the threshold. Action potential width was calculated as the time it took the membrane potential to reach half the spike amplitude in the rising part of the spike to the descending part of the spike (full-width at half-maximum).

Input conductance—The input conductance was calculated around the resting membrane potential by measuring the current with the cell held in voltage clamp mode first at −70 mV and then at −50 mV. The difference in currents divided by the difference in membrane potential (of 20 mV) is the calculated input conductance.

Sodium-to-potassium ratio—The sodium-to-potassium ratio was calculated as the ratio between the sodium current when holding the membrane potential at −20 mV in voltage clamp mode and the potassium current when holding the membrane at 20 mV in voltage clamp mode. The sodium current is obtained by subtracting the minimum current, representing the inward sodium current from the current after stabilizing from the transient sodium current. The sodium at −20 mV is then divided by the slow potassium (sustained) current at 20 mV. One reason for choosing these currents is that, at −20 mV, the gating currents are small and the measured sodium currents are close to the actual sodium currents. The second reason is that, at −20 mV, many sodium channels have opened. At 20 mV, on the other hand, many potassium channels have opened, but the depolarization is not too large, and most cells would have no problem sustaining this potential.

Sodium and potassium currents—The sodium and potassium currents were acquired in voltage clamp mode. Cells were held at −60 mV, and voltage steps of 400 ms were made

in the range of −90 to 80 mV. Currents were generally normalized by the cell capacitance. In the Li measurements, no normalization was performed, because of the large change in cell capacitance caused by the Li treatment.

Fast and slow potassium currents—The fast potassium current has been shown to be related to the A-type potassium channels.[54] We measured the fast potassium current by the maximum current immediately following a depolarization step, typically within a time window of a few milliseconds. The slow potassium currents were obtained at the end of the 400 ms depolarization step and have been shown to be related to the delayed rectifier potassium channels.[54]

Classification between NR and LR patients

The training set that was used for training the model was electrophysiological recordings taken during the 10–21 differentiation days, as the differences between the NR and LR neurons are largest at these times. The model was trained with features extracted from the recordings of five patients each time, and the classification was done on the sixth patient. This procedure was followed repeatedly for each of the six patients (training on the recordings of the other 5). The features that were used by the classifier were (1) the total number of spikes in 30 current injections, stating from 12 pA below the current needed to hold the cell at −60 mV; (2) the spike height; (3) the threshold potential for evoking an action potential; (4) the number of spikes in the first three current injection steps starting with the smallest current injection needed to produce one spike; (5) the number determined in the fourth feature normalized by the total number of spikes as in the first feature; (6) the number of spikes in the first three current injections as in the fourth feature divided by the number of spikes in the next three current injections; (7) the normalized sodium currents at −20 mV (normalized by cell capacitance); and (8) the fast potassium currents at 20 mV divided by the slow potassium currents at 20 mV. The features were quantized into two levels. The distribution of each of the features was learned on the training data set: $\Pr\{f_i = x_j | LR\} = \frac{\sum_m \delta[x_j/LR]}{\sum_j \sum_m \delta[x_j/LR]}$ and $\Pr\{f_i = x_j | NR\} = \frac{\sum_m \delta[x_j/NR]}{\sum_j \sum_m \delta[x_j/NR]}$, where m is the number of sample from the training set. The test set was the recordings of the remaining (new to the model) patient, whose samples were not used to train the model, We used an NB classifier, which assumes statistical independence between the features, and so the likelihood of obtaining features $f_1, f_2, \ldots, f_n$ from the positive or negative set is given by:

$$P_r\{f_1, f_2 \ldots f_n | LR\} = P_r\{f_1 | LR\} \times P_r\{f_2 | LR\} \times \ldots \times P_r\{f_n | LR\},\ P_r\{f_1, f_2 \ldots f_n | NR\} = P_r\{f_1 | NR\} \times P_r\{f_2 | NR\} \times \ldots \times P_r\{f_n | NR\}$$

We classified according to the maximal posterior probability and generated a score that was the ratio of the two posterior probabilities

$$P_r\{LR|f_1,f_2,\ldots f_n\} = \frac{P_r\{f_1,f_2,\ldots f_n|LR\} * P_r\{LR\}}{P_r\{f_1,f_2,\ldots f_n\}},$$

$$P_r\{NR|f_1,f_2,\ldots f_n\} = \frac{P_r\{f_1,f_2,\ldots f_n|NR\} * P_r\{NR\}}{P_r\{f_1,f_2,\ldots f_n\}}$$

Since when we have a new patient that we need to classify, we usually patch a few neurons, and we know *a priori* that these all belong to the same patient, we can use this information to improve prediction. We therefore multiply the posterior probabilities for classification of a few neurons, take the ratio and classify according to this score.

RESULTS

Differentiation of hippocampal DG-like neurons from EBV-immortalized B-lymphocytes from BD patients

Six patients with BD type I (three LR and three NR) were recruited as well as four healthy control subjects (see Materials and Methods for further details). The B-lymphocytes from these patients and neurotypical controls were immortalized using EBV virus and reprogrammed into iPSCs using the Yamanaka episomal vector set described by Okita *et al.* [53] (see Materials and Methods for more details). The iPSC clones that passed the quality controls described below in the Materials and Methods (Figure 1a–d) were differentiated into a primed neural progenitor cell population and subsequently into hippocampal DG granule-cell-like neurons using a protocol described previously[55] (Figure 1e and f). Over 48% of the differentiated neurons expressed the *Prox1* gene, which is a specific marker for dentate granule cells, and no significant difference was observed between controls and patients (average controls: 49.11 ± 6.30%; LR: 48.87 ± 5.23%; NR: 49.59 ± 6.37%, all errors given as s.e.m.) (Figure 1f). This demonstrates that reprogramming of EBV-immortalized B-lymphocytes into iPSCs was possible and that the differentiated cells could be used to obtain reliable data are important advances in the field because large collections of these cells are banked and readily accessible.

DG-like hippocampal neurons derived from BD patients are hyperexcitable, but the intrinsic properties of LR and NR neurons are profoundly different

We patch clamped Prox1::EGFP-expressing neurons at 3.5 weeks postdifferentiation from four control cell lines (95 cells), three LR patient cell lines (84 cells) and three NR patient cell lines (63 cells). Representative traces of evoked action potentials of control, LR and NR neurons are shown in Figure 2a–c. The neurons derived from both LR and NR patient cells were hyperexcitable, with an average of 21.2 ± 2.4 (control), 48 ± 5.5 (LR) and 48.7 ± 8.3 (NR) evoked action potentials ($P<0.0001$ for LR neurons vs control and $P = 0.0002$ for NR neurons vs control), producing more action potentials with injection of current (Figure 2d with a patient-by-patient plot in Figure 2e). The spontaneous firing rate was the highest in the LR group and lowest in the control group, with averages of 0.71 ± 0.14 Hz (LR), 0.35

± 0.08 Hz (NR) and 0.24 ± 0.06 Hz (control) firing rates (Figure 2f, $P = 0.0006$ LR vs control, $P = 0.28$ NR vs control and $P = 0.03$ LR vs NR). Averaging all BD lines together and comparing them with the control lines revealed a significance of $P = 0.0055$ BD vs control). Using voltage clamp mode, we recorded sodium and potassium currents. Representative traces are shown in Supplementary Figures 1c–e. The averages of the sodium currents are shown in Figure 2g; the fast and slow potassium currents are shown in Supplementary Figures 1a and b. We found that LR and control neurons exhibited similar sodium currents, but NR sodium currents were 45% lower (Figure 2g). There was no significant change in the potassium currents (Supplementary Figures 1a and b). The ratio between the sodium and potassium currents (see Materials and Methods) was 25% higher in LR (not significant) compared with control neurons and 46% lower ($P = 0.0006$) in NR neurons compared with control neurons (Figure 2h).

Spike shape is an important determinant of neuronal excitability. We therefore analyzed the spike shape for the three groups. Figure 2j–l displays representative traces of an action potential of LR, NR and control DG-like neurons recorded in current clamp mode. Figure 2i gives a schematic of the parameters analyzed for the spike shape. LR neuron spikes had increased amplitude of 20% ($P = 0.0006$) compared with control neurons, whereas NR neuron spikes had 15% lower amplitude than control neurons ($P = 0.01$) ($P<0.0001$ between LR and NR) (Supplementary Figure 1f). It should be noted that the spike height is correlated with the size of sodium currents, but this does not explain all the differences between subjects. Other factors that have an impact on the spike height are the sodium channels kinetics, the potential in which they open and the potential in which the potassium channels open. In addition, there are more factors, for example, the sodium currents are increased (at −40 mV, there is ~ 80%, $P = 0.15$ more sodium currents in the LR neurons than the controls), additionally the kinetics of the channels is faster (the rise time, the time it takes the spike to reach the maximum, is decreased in LR neurons and is 2.4 ± 0.2 ms in LR vs 2.8 ± 0.2 ms in controls, $P = 0.13$). The combination of faster channels that open at a less depolarized potential allow for the spike height to be significantly larger in LR neurons. It should also be noted that taking the area under the sodium currents curve from −60 to −20 mV is ~ 20% increased in LR neurons, similar to the increase in spike height. The fast 5-ms AHP was larger for BD neurons (but not significantly in this data set) (Supplementary Figure 1g). Spikes were 21% narrower in LR and 18% wider in NR compared with control neurons ($P = 0.0475$ control to LR, $P = 0.15$ control to NR and $P = 0.0002$ LR to NR) (Supplementary Figure 1h). The threshold for evoking a spike was 6 mV more depolarized in NR ($P<0.0001$ for both control to NR and LR to NR) (Supplementary Figure 1i). This finding seems at odds with the neurons' hyperexcitability, but excitability is a combination of many factors. For example, Down syndrome model neurons have been shown to have a less depolarized threshold, yet they are hypoexcitable.[56] Input conductance is also an important player in cell excitability.[57] A cell with lower conductance synaptic current inputs will cause a larger change in the membrane potential (through Ohm's law), so lower currents are needed to reach the threshold for spiking. There was no change to the input conductance in BD neurons (Supplementary Figure 1j). Capacitance was slightly increased for BD neurons (Supplementary Figure 1k) but not significantly in this data set.

Extending the measurement time frame further strengthens the results

To understand if the changes we observed for BD DG-like neurons appeared only during a narrow time window of cell maturation, we patch clamped the neurons from 10 to 45 days postdifferentiation, keeping the number of cells similar in each recording period between the three groups (control $n = 190$ cells from four lines, LR $n = 155$ cells from three lines and NR $n = 112$ cells from three lines). The number of evoked action potentials followed the BD general phenotype and was significantly increased for LR (37.5 ± 3.9) and NR (39.2 ± 5.4) DG-like neurons vs 20.6 ± 1.7 action potentials in control neurons ($P<0.0001$ for both LR vs control and NR vs control; Figure 3a). The sodium currents were similar for LR and control neurons but were ~ 45% lower for NR neurons ($P<0.0001$; Figure 3b). The fast potassium currents were ~ 8% increased in LR compared with control neurons (0 = 0.014, two-way analysis of variance) and ~ 5% increased in LR neurons compared with NR neurons ($P = 0.0085$) (Figure 3c). The slow potassium currents did not change between the three groups (Figure 3d). The sodium-to-potassium ratio was 42% reduced in NR neurons compared with control ($P = 0.0002$) and LR neurons ($P = 0.0006$) (Figure 3e). Capacitance was slightly increased in LR neurons, but a significant difference was seen in NR neurons ($P = 0.038$) (Figure 3f). Cell input conductance did not change between the three groups (Figure 3g). Spike shape differed between the three groups: LR neurons had a higher spike amplitude (+17% $P = 0.0002$), whereas NR had a smaller spike amplitude compared with controls (−13%, $P = 0.01$) (Figure 3h). As noted in the previous section, the combination of channels that have stronger currents at −40 mV (86% increase in LR neurons compared with controls, $P = 0.02$) and a faster kinetics gave rise to a bigger amplitude spike. If we look at the area under the curve of the sodium currents from −60 to −20 mV, it is increased by 19%, similar to the increase in spike height. The 5-ms AHP amplitude was larger in LR neurons (+21%, $P = 0.03$) than in control neurons and was even larger in NR neurons (+49% $P = 0.0003$) (Figure 3i). Spike width was the narrowest in LR and widest in NR neurons, with a significant difference between NR and LR neurons (+21%, $P = 0.03$) (Figure 3j). The threshold for firing was 6 mV higher (more depolarized) in NR neurons compared with the other two groups ($P<0.0001$ NR to control, $P<0.0001$ NR to LR) (Figure 3k). We found that the distinct features of LR and NR neurons vs control neurons that were evident at 3.5 weeks differentiation were observed through the entire measurement period of 10– 45 days postdifferentiation, and the significance of the results increased in all measured parameters (except for spike width) when analyzing the entire data set. Remarkably, while the endophenotype of hyperexcitability is shared between NR and LR neurons, their difference from the control neurons is in almost all parameters tested (except for the large fast AHP) in an opposite direction.

Predicting a patient's responsiveness to Li according to electrophysiological measurements

As our results indicated that NR and LR neurons have very different electrophysiological properties, we next wondered if we could predict the patient's response to Li based only on electrophysiological measurements from its derived neurons. To make these findings applicable for medical purposes, we separated the data into training data composed of recordings of five patients (see Figure 4a), and then classified recordings from a patient who was new to the model (see Figure 4b). We used an NB classifier (see Materials and

Methods), which learns the posterior probabilities of features extracted from the electrophysiological measurements given that the patient was an NR or LR patient. This model was then used to classify the remaining patient (see Figure 4b). Performance was assessed by repeating this process 2000 times and the patient left out of the training data was a different patient each time. Since a patch-clamp recording session usually consists of patching a few neurons, to improve performance, we used, as the test data, 1-, 3- or 5-cell recordings (from 1 or 3 or 5 cells accordingly, see Materials and Methods). The recordings were chosen randomly from the recordings of the patient being classified, and this procedure was repeated randomly 2000 times to get a statistical estimate of the success rate. When classifying patient SBP001 (NR) according to one patch clamped neuron, the success rate was 76%; classifying according to 3-cell recordings gave a success rate of 83%, and with 5-cell recordings, the success rate was 92%. When classifying patient SBP002 (NR) with a 1-neuron recording, the success rate was 88%; with 3-cell recordings, the success rate was 100%, and with 5-cell recordings it was 100% as well. When classifying patient SBP004 (NR) with 1-neuron recordings, the success rate was 62%; with 3-cell recordings, the success rate was 81%, and with 5-cell recordings it was 88%. When classifying patient SBP005 (LR) with 1-neuron recordings, the success rate was 67%; with 3-cell recordings, the success rate was 81%, and with 5-cell recordings it was 90%. When classifying patient SBP007 (LR) with 1-neuron recording, the success rate was 73%; with 3-cell recordings the success rate was 76%, and with 5-cell recordings it was 85%. When classifying patient SBP010 (LR) with 1-neuron recordings, the success rate was 82%; with 3-cell recordings, the success rate was 97%, and with 5-cell recordings it was 100%. The performance was further assessed by calculating the receiver-operating characteristics curve for classification according to a single neuron recordings, 3-cell recordings or 5-cell recordings (see Figure 4c), where the area under the curve was 0.81, 0.94 and 0.98, respectively. To summarize, having obtained electro-physiological measurements of a new patient, we can predict with excellent accuracy whether this patient will respond well to Li treatment.

Analysis of the most excitable cells of control, LR and NR neurons Since the most obvious phenotype for both LR and NR neurons is their hyperexcitability, we characterized the most excitable neurons in each group and compared their electrophysiological profiles. We characterized a subset of the data of neurons that had at least 35 evoked action potentials (termed ‘hyper’) in all depolarization steps in 400 ms recording (see Materials and Methods) and compared it with the remaining part of the data (termed ‘hypo’). In the control group, there were 34 ‘hyper’ of the 190 cells (18%), with an average of 58.3 ± 4.2 action potentials (compared with 11.6 ± 0.7 in the control hypo $P<0.0001$), whereas for the LR neurons there were 60 ‘hyper’ of the 155 cells (39%), with an average of 79.9 ± 7 action potentials (compared with 10.7 ± 1 in the LR ‘hypo’ $P<0.0001$), and 37 ‘hyper’ of the 112 of the NR neurons (33%), with an average of 106.8 ± 10.5 action potentials (compared with 10.1 ± 1.1 $P<0.0001$) (Figure 5a compares the ‘hyper’ vs ‘hypo’ neurons in each of the three groups; Supplementary Figure 2a makes two comparisons: the ‘hyper’ neurons of each of the three groups and the ‘hypo’ neurons of each of the three groups). Sodium currents were higher in all the groups in the ‘hyper’ vs ‘hypo’ groups (at the maximum current, control increased by 85% $P<0.0001$, LR increased by 96% $P<0.0001$, NR increased by 112% $P = 0.0004$). The NR neurons had the lowest sodium currents in all the hyper and hypo groups (Figure 5b).

The fast potassium currents were increased between control 'hyper' and 'hypo' neurons by ~ 15% ($P = 0.015$, two-way analysis of variance; Figure 5c). In LR, the increase was ~ 10% ($P = 0.006$). For the NR neurons, there was no significant increase in the fast AHP. The changes in the slow potassium currents between the 'hyper' groups and the 'hypo' groups are shown in Figure 5d. There was no significant change between any of the pairs. The sodium-to-potassium ratio in the 'hyper' vs 'hypo' sets of the data was larger in all groups by ~ 56% control ($P<0.0001$), 112% LR ($P<0.0001$) and 102% NR groups ($P<0.0001$, Figure 5e and Supplementary Figure 2b). Another interesting phenomenon (Figure 5e and Supplementary Figure 2b) was that there were both 'hyper' LR and NR neurons with a ratio of sodium-to potassium close to 0 (but not the controls), indicating that BD neurons can be hyperexcitable even with very low sodium-to-potassium ratio. The capacitance was larger in the 'hyper' groups of the control and LR (59% control, $P<0.0001$ and 24% LR, $P = 0.0002$), confirming a reduced correlation between capacitance and excitability in NR neurons (Figure 5f and Supplementary Figure 2c). The input conductance of the neurons generally did not change between the 'hyper' groups and 'hypo' groups (an increase of 40% in the control 'hyper' vs 'hypo' cells, $P = 0.05$, Figure 5g and Supplementary Figure 2d).

Analysis of the spike shape for the 'hyper' vs 'hypo' groups revealed that the spike amplitude increased by 53% in the controls ($P<0.0001$), 30% in LRs ($P<0.0001$) and 55% in NRs (Figure 5h and Supplementary Figure 2e). A big change was observed in the 5-ms AHP when comparing the 'hyper' and 'hypo' neurons in all three groups. Controls exhibited an increase of 196% ($P<0.0001$), LRs 123% ($P<0.0001$) and NRs 85% ($P<0.0001$, Figure 5i and Supplementary Figure 2f). The spike width of the 'hyper' neurons was narrower than that of the 'hypo' neurons (−60% in control $P<0.0001$, − 46% in LR $P<0.0001$ and − 43% in NR $P<0.0001$) (Figure 5j and Supplementary Figure 2g). The threshold for firing was less depolarized in the 'hyper' vs 'hypo' neurons (3.3 mV for control neurons $P = 0.0012$, 3.8 mV for LR neurons $P = 0.005$ and 5.6 mV for NR neurons $P<0.0001$), with the NR neurons having a more depolarized threshold in both the 'hyper' and 'hypo' groups (Figure 5k and Supplementary Figure 2h).

To summarize, the functional features that characterize the hyperexcitable neurons include larger sodium currents that open at a less depolarized potential (~ −50 mV), larger fast potassium currents that also open at a less depolarized potential (~ −30 mV), larger sodium-to-potassium ratio and a larger capacitance. The typical spike shape of the hyperexcitable neurons is a larger amplitude narrower spike with a less depolarized threshold for evoking an action potential and a very large increase in the fast AHP amplitude. While these features characterize a hyperexcitable neuron, the diversity of these features within the population changes in the three groups of control, LR and NR neurons. The control neurons changes between the 'hyper' and 'hypo' neurons, is most pronounced in the fast AHP, whereas in the NR group the largest changes are found in the sodium currents when comparing 'hyper' and 'hypo' neurons. The LR group changes in the sodium and fast AHP between 'hyper' and 'hypo' neurons are somewhere between the control and NR groups. The differences in the basic features and currents between the three groups of control, LR and NR neurons, may explain not only the average larger excitability of NR and LR neurons but also the larger diversity of the BD, and especially NR BD, excitability phenotype. For example, the total number of evoked action potentials in the NR neurons for the entire data set was 39.2 ± 5.4,

whereas it was 20.6 ± 1.7 in the controls, with the average larger, but also a much larger coefficient of variation in the NR group (0.14 NR vs 0.08 control).

Hyperexcitability is reversed by chronic Li treatment of LR DG-like neurons but not of NR neurons, and Li treatment reduces cell capacitance in both LR and NR neurons

Mertens *et al.*[42] reported differential responses to Li depending on whether the neurons were derived from LR or NR patients. To test Li responsiveness in our cells, we chronically treated neurons with 1 mM LiCl (see Materials and methods). Neuronal excitability, as defined by the total evoked action potential, was reduced in neurons from LR patients (59 non-treated cells and 67 treated cells from three cell lines, a reduction of 40% in the total number of evoked spikes in 30 depolarization steps, $P = 0.02$) but not in neurons from NR patients (44 non-treated cells and 47 treated cells from three cell lines, a reduction of 15% in the total number of evoked action potentials, $P = 0.44$) upon Li treatment (Figure 6a and i, with representative traces in current clamp mode shown in Figure 6b and j). Representative traces in voltage clamp mode of sodium and potassium currents are shown in Supplementary Figure 3a (LR), 3b (LR Li), 3 h (NR) and 3i (NR Li). The sodium current at −20 mV is shown in the inset of each figure. The sodium currents were reduced in LR neurons after Li treatment by ~ 10% ($P = 0.03$, two-way analysis of variance) but not in NR neurons (Figure 6c and k). Although the average across sodium currents in all holding potentials was reduced in LR neuron in response to Li treatment, the spike height was not expected to change, as at −60 to −20 mV there was no change to the sodium currents, and these are the potentials that influence mostly the spike height. The fast potassium currents were reduced by ~ 13% ($P = 0.0078$) and by ~ 6% in NR neurons ($P = 0.005$) (Figure 6d and l). The slow potassium currents did not change (Figure 6e and m).

Analysis of the action potential shape revealed that chronic Li treatment also changed the action potential characteristics. Representative traces of an action potential acquired in current clamp mode are shown in Figure 6f (red, LR), 6 g (orange, LR lithium), 6n (purple, NR) and 6o (pink, NR lithium). Following chronic Li treatment, the spike amplitude did not change in either LR or NR DG-like neurons, although there was some reduction in the sodium currents of LR neurons, but this reduction was not very large in the − 60 to − 20 mV range, which is the range that affects the spike amplitude (Supplementary Figures 3c and j). The fast AHP amplitude decreased in both LR (−30%, $P = 0.029$) and NR neurons (−40%, $P = 0.02$) (Supplementary Figures 3d and k). The spike width broadened in the LR neurons (36%, $P = 0.03$), with an effect in the same direction in NR neurons (Supplementary Figures 3e and l), and the threshold for firing decreased in the NR neurons (3 mV less depolarized, $P = 0.04$) with an effect in the same direction in LR neurons (Supplementary Figures 3f and m). The input conductance did not change for either cell type (Supplementary Figures 3g and n). Interestingly, the effect of Li on both LR and NR neurons is similar, but the final effect depends on the cell's initial properties. Therefore, Li acts in two different ways: on the one hand, it decreases fast AHP amplitude and broadens the spike; on the other hand, it reduces the threshold for evoking an action potential and increases the sodium currents around −40 mV. This dual form of action might be the mechanism that allows Li to improve symptoms in both mania and depression phases. The final significance of the effect of Li depends on the original properties of the cells. For example, LR spikes are very narrow, and

after Li treatment they become significantly broader, whereas NR spikes are broad to begin with and become broader with Li, but not significantly. While the final significant effects of Li treatment on the spike shape of LR neurons are both in the direction of reduced excitability (the fast AHP amplitude decreases and the spike broadens), the effect on the spike shape of NR neurons is in an antagonist direction; the fast AHP amplitude decreases, which reduces excitability, but the threshold for evoking an action potential is less depolarized, and this has the effect of increasing cell excitability, resulting in a similar number of hyperexcitable neurons after Li treatment.

Surprisingly, Li treatment caused a significant reduction in the cell capacitance for both LR (−23%, $P = 0.0022$, Figure 6h) and NR (−30%, $P = 0.0016$, Figure 6p) neurons. The cell capacitance is proportional to the total area of the membrane, and a reduction may be related to a smaller cell body or fewer branched dendrites/axons. To understand how cell capacitance correlates with excitability, we plotted the total number of spikes vs the capacitance (Supplementary Figures 3o–q, for control, LR and NR, respectively). The Pearson's correlation for control cells and LR cells was 0.44, whereas for NR cells the correlation was 0.26. Li had the effect of slowing the cell growth and subsequent size, suggesting another explanation of how NR neurons are less affected by Li treatment. While smaller LR neurons are less excitable, smaller NR neurons can be hyperexcitable, as shown by the reduced correlation between cell capacitance and excitability in NR neurons.

It was also interesting to observe how Li affected the different populations of hyperexcitable vs hypoexcitable neurons for LR and NR groups. Before Li treatment, 59% of the neurons were hyperexcitable in the LR group; after treatment, only 35% were hyperexcitable. In the NR group, 50% of the neurons were hyperexcitable before treatment, whereas after treatment the change was not marked and 47% were hyperexcitable. Although it seems that Li had almost no effect on NR neurons, it is not clear if this was the case or if there was a switching of neurons from the hyperexcitable NR group to the hypoexcitable NR group and *vice versa*. It is clear that more neurons shifted from the hyperexcitable group to the hypoexcitable group for the LR neurons. Note that in the Li treatment analysis, neurons at 22–30 days of differentiation were recorded, and hence the larger number of 'hyper' neurons compared to the previous section, where neurons were recorded and analyzed throughout the entire differentiation period.

Analysis revealed that sodium currents of hyperexcitable neurons opened at a lower potential in both LR and NR neurons. The sodium currents that were measured at −40 mV, which have a large influence on cell excitability since they are close to the potential needed for evoking an action potential, changed with Li treatment. Increases of 257% $P = 0.01$ in LR neurons and 228% $P = 0.07$ in NR neurons were observed. The effect was in opposite directions in the 'hypo' neurons between LR and NR neurons (a decrease of 60%, $P = 0.08$, in the LR neurons vs an increase of 193%, $P = 0.26$, in NR neurons) (Supplementary Figure 4a and b). Cell capacitance decreased in the hypoexcitable LR neurons (29% decrease, $P = 0.0015$), whereas in the NR neurons the cell capacitance decreased in both the hyperexcitable cells (26% decrease, $P = 0.03$) and the hypoexcitable cells (39%, $P = 0.004$) (Supplementary Figure 4g and h). No significant differences were observed between fast and slow potassium currents or the spike height when comparing the Li-treated neurons in the

'hyper' vs 'hypo' excitable neurons of the LR and NR groups (Supplementary Figure 4c–f). The amplitude of the fast AHP of the hyperexcitable neurons was reduced in both the LR and NR neurons (a decrease of 23%, $P = 0.05$ for LR 'hyper' neurons, and a decrease of 30%, $P = 0.01$ for 'hyper' NR neurons); no significant change was seen in the 'hypo' LR and NR neurons (Supplementary Figure 4k and l). Although there were no significant differences observed in spike width when comparing the Li-treated neurons in the 'hyper' vs 'hypo' excitable neurons of the LR and NR groups, keeping in mind that the overall effect of Li is broadening of the spike in the LR group, neurons with a broader spike had shifted to the 'hypo' group (Supplementary Figure 4m and n). The threshold was less depolarized in the 'hyper' neurons of the LR group (5 mV less depolarized, $P = 0.025$). In the NR group, the effect was in the 'hypo' group (4.9 mV less depolarized after Li treatment, $P = 0.037$). While it is hard to draw clear conclusions from these data—as we can only look at Li-untreated and -treated cells but not at the same cell with/without Li treatment and we therefore do not know if there was an exchange of cells between the 'hyper' and 'hypo' groups—there are some strong hypotheses that can be proposed. It appears that Li shifts many more 'hyper' state cells to the 'hypo' state in the LR group, whereas in the NR group the shift seems to be in both directions, resulting in a similar number of cells that are hyperexcitable after Li treatment. For both NR and LR neurons, Li generally decreases the fast AHP and broadens the spike but opens the sodium channels at a lower (less depolarized) potential. The final effect depends very much on the initial properties of the cell. For example, in the NR neurons, as the sodium channels are much less open at − 40 mV than in the LR neurons, this opening of the channels due to the Li treatment may help in the shift of many neurons to the 'hyper' state, whereas this effect is less strong in the LR neurons.

DISCUSSION

In this study, we present functional measurements of DG granule-cell-like neurons differentiated from iPSCs derived from EBV-immortalized lymphocytes of BD patients. We find that the endophenotype of hyperexcitability is shared by BD DG neurons, in support of our previous findings.[42] We further show that BD neurons can be subdivided into at least two populations of neurons, where neurons within a sub-population share similar features but these sub-populations are very different functionally from each other. Using features extracted from electrophysiological measurements from these two sub-populations, can predict the responsiveness of a new patient to Li with a success rate of over 92%. The cellular phenotype shared by these sub-populations is hyperexcitability, and the electrophysiological feature that they share is a large fast AHP, a feature known to assist fast spiking interneurons with their fast spiking abilities.

Fast spiking neocortical interneurons can produce very high frequency firing rates. Their electrophysiological properties include a high amplitude, narrow spike and a large fast AHP.[58–60] Fast AHP is known to assist rapid recovery of Na^+ channel inactivation,[61] allowing for a high persistent rate of firing. Interestingly, our first sub-population of BD neurons, the LR neurons, displayed a similar phenotypic behavior to fast spiking interneurons—a high amplitude, narrow spike, with a large fast AHP—that explains their hyperexcitability and fast spiking abilities. The other sub-population of BD neurons, the NR neurons, were very different from both the first population (LR) and from the control neurons. They had a

smaller spike amplitude and a wider spike, and they exhibited an almost 50% reduction in sodium currents along with a more depolarized threshold. The large differences between the two subgroups of BD neurons suggest two distinct subdisorders, with very different intrinsic properties, where the common cellular phenotype is hyperexcitability. Their shared electrophysiological feature, a large fast AHP, suggests a possible expedited recovery of sodium channel inactivation, which allows BD neurons to sustain spiking activity. When looking for examples of fast or slow spiking neurons, it is useful to observe the other end of the spectrum as well. Down Syndrome neurons, which are hypoexcitable, have a very small amplitude of the fast AHP.[56]

The functional profile was measured over the 3.5-week time period (Figure 2) and then repeated over a very wide maturation period (keeping the ratios of cells in each time period similar; Figure 3). The features measured in the short recording period were preserved over the longer recording period, almost as if they were keeping some special developmental program. Thus, for example, the NR sub-population had reduced sodium currents at 2 and 6 weeks after the start of differentiation. This larger data set allowed us to see more differences through the large biological noise, and strengthened the significance of some other differences. Again, we observed that NR neurons were hyperexcitable and were characterized by a wider, lower amplitude spike, with a more depolarized threshold for spiking and a higher amplitude fast AHP. The NR neurons had lower sodium currents at all stages of maturation. Their capacitance was larger than that of both the other groups (with a significant results compared with controls). LR neurons were hyperexcitable and were characterized by a narrower, higher amplitude spike and a higher amplitude fast AHP at all stages of maturation. The resemblance in the spike shape of the LR to that of fast spiking interneurons suggests immediately that they too will have properties of fast spiking abilities. The NR neurons, on the other hand, have the large fast AHP feature but also have reduced sodium currents. These differences hint at what may be a more complicated phenotype of hyperexcitability, with a possible change to hypoexcitability because of changes in the cell or its environment, or by the natural diversity throughout a population.

The features of NR and LR neurons were so different that they led us to believe that the patient’s responsiveness to Li could be predicted based on electrophysiological measurements alone. We therefore constructed an NB model that trained on five patients and predicted a new patient’s response to Li with a remarkable accuracy and with an area under the curve of 0.98 using an receiver-operating characteristics curve, where features used for classification were extracted from 3- or 5-cell recordings (Figure 4). These findings not only strengthen the observation that NR and LR neurons have very different intrinsic properties but also may have direct medical applicability for any new patient who needs to be classified as LR or NR.

We proceeded to characterize the most excitable neurons from each group (see Materials and Methods for definition of the most excitable neurons). Generally, the more excitable neurons, which we termed ‘hyper’ neurons, had larger sodium currents that opened at a less depolarized potential (Figure 5b) compared with the ‘hypo’ neurons. The fast potassium currents were also 10–15% higher in the control and LR ‘hyper’ groups, compared with the matching ‘hypo’ neurons (Figure 5c), and generally in the more excitable neurons the fast

potassium channels opened in a less depolarized potential. The sodium-to-potassium ratio was larger for the ‘hyper’ neurons of all three groups (Figure 5e), indicating that this ratio of the sodium currents at −20 mV (approximately the potential where the sodium channels opened) to the potassium currents at 20 mV (a potential where many of the potassium channels have opened, close to the peak of the action potential) is an important feature of cell excitability. Interestingly, only BD neurons were hyperexcitable when the sodium-to-potassium ratio was close to 0 (Figure 5e), indicating that another cell-intrinsic property had a role. The capacitance of the ‘hyper’ neurons was larger in the control and LR groups compared with the ‘hypo’ neurons. There was no significant change in the capacitance of the ‘hyper’ NR neurons, strengthening the observation of weaker correlation between excitability and capacitance in the NR group. In contrast, the input conductance was generally not a main feature distinguishing between our ‘hyper’ and ‘hypo’ neurons in our DG neurons. The spike of the ‘hyper’ neurons was narrower, with a larger amplitude in all three groups. The fast AHP was larger for ‘hyper’ neurons, and the threshold was less depolarized (Figures 5h–k). Interestingly, the largest difference in the spike shape was attributed to the fast AHP, with a ~ 3-fold change in the control group from the ‘hypo’ to the ‘hyper’ types and an ~ 2-fold change in the LR and NR groups, indicating that the fast AHP was an important determinant of cell hyperexcitability. This lower change in fast AHP in the BD neurons suggested that BD neurons were already primed for the next action potential through fast recovery from sodium inactivation.

An important validation of these cells as model BD neurons is their response to drugs, specifically Li. Our results demonstrate that, similar to our previous report with fibroblast-derived neurons,[42] the neurons derived from LR patients responded to Li by decreasing their hyperexcitability but the neurons from the NR group did not (Figures 6a and i). A surprising result was the reduction in the cell capacitance with Li treatment for both the LR and NR neurons (Figures 6h and p). The cell capacitance is proportional to the total area of the membrane, and a reduction may be related to a smaller cell body or fewer branched dendrites/axons. NR neurons have a lower correlation between excitability and capacitance (Supplementary Figures 3o–q), thus despite this decrease in cell capacitance with Li treatment, the NR neurons could be hyperexcitable. The reduced correlation in NR neurons between excitability and cell capacitance may point to some dysregulation between the growth rate of the neuron and ion channel expression in the NR neurons.

It is interesting to note that Li had a ‘dual’ effect on the cells. It both reduced the amplitude of the fast AHP and broadened the spike, making the cells less excitable, but it also caused the sodium channels to open at a less depolarized potential, making the cells more excitable. We hypothesize that this may be the way in which Li has a dual action of improving both depression and mania. The significance of the effect on the types of cells (LR vs NR) depends on their initial properties. The significant changes that occurred in the action potential shape of LR neurons (broadening of the spike and reduction of the fast AHP amplitude; Supplementary Figures 3d and e) generally reduced excitability in neurons, whereas the significant changes in the NR neurons after Li treatment contributed in a different direction to cell excitability (spike broadening decreased excitability, whereas lowering the threshold increased excitability; Supplementary Figures 3k and m).

To summarize, we have demonstrated that iPSCs can be derived from EBV-immortalized B-lymphocytes and that these iPSCs can be differentiated into DG-like neurons. We reproduced the reported endophenotype of hyperexcitability in DG neurons from a new cohort of BD patients and cells. We showed that BD neurons originating from LR and NR patients create two sub-populations of cells that are so intrinsically different from each other that it is possible to predict the response of a new patient to Li based on electrophysiological recordings alone. The large fast AHP that all BD neurons share suggests that it is a key to their repetitive spiking abilities and their hyperexcitability, similar to reports on other types of neurons in which a large fast AHP contributes to fast spiking abilities, such as the fast spiking interneurons.

Supplementary Material

Refer to Web version on PubMed Central for supplementary material.

Acknowledgments

We thank Mary Lynn Gage for help with editing the article, Elisha Moses and Menahem Segal for very helpful discussions and L Moore, E Mejia and B Miller for technical assistance. SBP thanks Haowen Zhou for technical assistance, Drs Michael Jackson, Ian Pass, Guang Chen, Evan Snyder, Andrew Crane and Brian Tobe for discussion of line selection, and Drs Dongmei Wu and Yang Liu at the SBP Stem Cell Core. SBP acknowledges support from the Viterbi Family Foundation of the Jewish Community Foundation San Diego. For the production of the iPSCs, SBP would like to acknowledge financial support from Janssen Pharmaceuticals. The production of neural progenitor cells and electrophysiological measurements were also supported by Janssen Pharmaceuticals. The collection of clinical data and lymphoblasts was supported by the Grant No. 64410 from the Canadian Institutes of Health Research (CIHR) (to MA). This work was also supported by the Paul G Allen Family Foundation, Bob and Mary Jane Engman, The Leona M and Harry B Helmsley Charitable Trust Grant No. 2012-PG-MED002, Annette C Merle-Smith, R01 MH095741 (to FHG), U19MH106434 (to FHG) and by The G Harold and Leila Y Mathers Foundation.

References

1. Angst J. The emerging epidemiology of hypomania and bipolar II disorder. J Affect Disord. 1998; 50:143–151. [PubMed: 9858074]
2. Hirschfeld RM, Calabrese JR, Weissman MM, Reed M, Davies MA, Frye MA, et al. Screening for bipolar disorder in the community. J Clin Psychiatry. 2003; 64:53–59.
3. Merikangas KR, Akiskal HS, Angst J, Greenberg PE, Hirschfeld RM, Petukhova M, et al. Lifetime and 12-month prevalence of bipolar spectrum disorder in the National Comorbidity Survey replication. Arch Gen Psychiatry. 2007; 64:543–552. [PubMed: 17485606]
4. Belmaker RH. Bipolar disorder. N Engl J Med. 2004; 351:476–486. [PubMed: 15282355]
5. Judd LL, Akiskal HS, Schettler PJ, Endicott J, Maser J, Solomon DA, et al. The long-term natural history of the weekly symptomatic status of bipolar I disorder. Arch Gen Psychiatry. 2002; 59:530–537. [PubMed: 12044195]
6. Vandeleur CL, Merikangas KR, Strippoli MP, Castelao E, Preisig M. Specificity of psychosis, mania and major depression in a contemporary family study. Mol Psychiatry. 2014; 19:209–213. [PubMed: 24126925]
7. Baethge C, Baldessarini RJ, Freudenthal K, Streeruwitz A, Bauer M, Bschor T. Hallucinations in bipolar disorder: characteristics and comparison to unipolar depression and schizophrenia. Bipolar Disord. 2005; 7:136–145. [PubMed: 15762854]
8. Harris EC, Barraclough B. Suicide as an outcome for mental disorders. A meta-analysis. Br J Psychiatry. 1997; 170:205–228. [PubMed: 9229027]
9. Tondo L, Isacsson G, Baldessarini R. Suicidal behaviour in bipolar disorder: risk and prevention. CNS Drugs. 2003; 17:491–511. [PubMed: 12751919]

10. Geddes JR, Burgess S, Hawton K, Jamison K, Goodwin GM. Long-term lithium therapy for bipolar disorder: systematic review and meta-analysis of randomized controlled trials. Am J Psychiatry. 2004; 161:217–222. [PubMed: 14754766]
11. Burgess S, Geddes J, Hawton K, Townsend E, Jamison K, Goodwin G. Lithium for maintenance treatment of mood disorders. Cochrane Database Syst Rev. 2001(3):CD003013.
12. Klein PS, Melton DA. A molecular mechanism for the effect of lithium on development. Proc Natl Acad Sci USA. 1996; 93:8455–8459. [PubMed: 8710892]
13. Jope RS. Anti-bipolar therapy: mechanism of action of lithium. Mol Psychiatry. 1999; 4:117–128. [PubMed: 10208444]
14. Chiu CT, Wang Z, Hunsberger JG, Chuang DM. Therapeutic potential of mood stabilizers lithium and valproic acid: beyond bipolar disorder. Pharmacol Rev. 2013; 65:105–142. [PubMed: 23300133]
15. Machado-Vieira R, Manji HK, Zarate CA Jr. The role of lithium in the treatment of bipolar disorder: convergent evidence for neurotrophic effects as a unifying hypothesis. Bipolar Disord. 2009; 11(Suppl. 2):92–109. [PubMed: 19538689]
16. Breen MS, White CH, Shekhtman T, Lin K, Looney D, Woelk CH, et al. Lithium-responsive genes and gene networks in bipolar disorder patient-derived lymphoblastoid cell lines. Pharmacogenom J. 2016; 16:446–453.
17. Viguera AC, Tondo L, Baldessarini RJ. Sex differences in response to lithium treatment. Am J Psychiatry. 2000; 157:1509–1511. [PubMed: 10964872]
18. Tohen M, Greil W, Calabrese JR, Sachs GS, Yatham LN, Oerlinghausen BM, et al. Olanzapine versus lithium in the maintenance treatment of bipolar disorder: a 12-month, randomized, double-blind, controlled clinical trial. Am J Psychiatry. 2005; 162:1281–1290. [PubMed: 15994710]
19. Smoller JW, Finn CT. Family, twin, and adoption studies of bipolar disorder. Am J Med Genet C. 2003; 123C:48–58.
20. McGuffin P, Rijsdijk F, Andrew M, Sham P, Katz R, Cardno A. The heritability of bipolar affective disorder and the genetic relationship to unipolar depression. Arch Gen Psychiatry. 2003; 60:497–502. [PubMed: 12742871]
21. Kieseppa T, Partonen T, Haukka J, Kaprio J, Lonnqvist J. High concordance of bipolar I disorder in a nationwide sample of twins. Am J Psychiatry. 2004; 161:1814–1821. [PubMed: 15465978]
22. International Schizophrenia C, Purcell SM, Wray NR, Stone JL, Visscher PM, O'Donovan MC, et al. Common polygenic variation contributes to risk of schizophrenia and bipolar disorder. Nature. 2009; 460:748–752. [PubMed: 19571811]
23. Craddock N, Sklar P. Genetics of bipolar disorder. Lancet. 2013; 381:1654–1662. [PubMed: 23663951]
24. Psychiatric GCBDWG. Large-scale genome-wide association analysis of bipolar disorder identifies a new susceptibility locus near ODZ4. Nat Genet. 2011; 43:977–983. [PubMed: 21926972]
25. Ferreira MA, O'Donovan MC, Meng YA, Jones IR, Ruderfer DM, Jones L, et al. Collaborative genome-wide association analysis supports a role for ANK3 and CACNA1C in bipolar disorder. Nat Genet. 2008; 40:1056–1058. [PubMed: 18711365]
26. Carter CJ. Multiple genes and factors associated with bipolar disorder converge on growth factor and stress activated kinase pathways controlling translation initiation: implications for oligodendrocyte viability. Neurochem Int. 2007; 50:461–490. [PubMed: 17239488]
27. Ogden CA, Rich ME, Schork NJ, Paulus MP, Geyer MA, Lohr JB, et al. Candidate genes, pathways and mechanisms for bipolar (manic-depressive) and related disorders: an expanded convergent functional genomics approach. Mol Psychiatry. 2004; 9:1007–1029. [PubMed: 15314610]
28. Nestler EJ, Hyman SE. Animal models of neuropsychiatric disorders. Nat Neurosci. 2010; 13:1161–1169. [PubMed: 20877280]
29. Einat H, Manji HK. Cellular plasticity cascades: genes-to-behavior pathways in animal models of bipolar disorder. Biol Psychiatry. 2006; 59:1160–1171. [PubMed: 16457783]
30. Rajkowska G, Halaris A, Selemon LD. Reductions in neuronal and glial density characterize the dorsolateral prefrontal cortex in bipolar disorder. Biol Psychiatry. 2001; 49:741–752. [PubMed: 11331082]

31. Bertolino A, Frye M, Callicott JH, Mattay VS, Rakow R, Shelton-Repella J, et al. Neuronal pathology in the hippocampal area of patients with bipolar disorder: a study with proton magnetic resonance spectroscopic imaging. Biol Psychiatry. 2003; 53:906–913. [PubMed: 12742678]
32. Bouras C, Kovari E, Hof PR, Riederer BM, Giannakopoulos P. Anterior cingulate cortex pathology in schizophrenia and bipolar disorder. Acta Neuropathol. 2001; 102:373–379. [PubMed: 11603813]
33. Rajkowska G. Postmortem studies in mood disorders indicate altered numbers of neurons and glial cells. Biol Psychiatry. 2000; 48:766–777. [PubMed: 11063973]
34. Cotter D, Mackay D, Landau S, Kerwin R, Everall I. Reduced glial cell density and neuronal size in the anterior cingulate cortex in major depressive disorder. Arch Gen Psychiatry. 2001; 58:545–553. [PubMed: 11386983]
35. Askland K, Read C, Moore J. Pathways-based analyses of whole-genome association study data in bipolar disorder reveal genes mediating ion channel activity and synaptic neurotransmission. Hum Genet. 2009; 125:63–79. [PubMed: 19052778]
36. Mahmood T, Silverstone T. Serotonin and bipolar disorder. J Affect Disord. 2001; 66:1–11. [PubMed: 11532527]
37. Scarr E, Pavey G, Sundram S, MacKinnon A, Dean B. Decreased hippocampal NMDA, but not kainate or AMPA receptors in bipolar disorder. Bipolar Disord. 2003; 5:257–264. [PubMed: 12895203]
38. Benes FM, Berretta S. GABAergic interneurons: implications for understanding schizophrenia and bipolar disorder. Neuropsychopharmacology. 2001; 25:1–27. [PubMed: 11377916]
39. Guidotti A, Auta J, Davis JM, Di-Giorgi-Gerevini V, Dwivedi Y, Grayson DR, et al. Decrease in reelin and glutamic acid decarboxylase67 (GAD67) expression in schizophrenia and bipolar disorder: a postmortem brain study. Arch Gen Psychiatry. 2000; 57:1061–1069. [PubMed: 11074872]
40. Fattal O, Link J, Quinn K, Cohen BH, Franco K. Psychiatric comorbidity in 36 adults with mitochondrial cytopathies. CNS Spectrums. 2007; 12:429–438. [PubMed: 17545953]
41. Marazziti D, Baroni S, Picchetti M, Landi P, Silvestri S, Vatteroni E, et al. Psychiatric disorders and mitochondrial dysfunctions. Eur Rev Med Pharmacol Sci. 2012; 16:270–275. [PubMed: 22428481]
42. Mertens J, Wang QW, Kim Y, Yu DX, Pham S, Yang B, et al. Differential responses to lithium in hyperexcitable neurons from patients with bipolar disorder. Nature. 2015; 527:95–99. [PubMed: 26524527]
43. Harrison PJ, Cader MZ, Geddes JR. Reprogramming psychiatry: stem cells and bipolar disorder. Lancet. 2016; 387:823–825. [PubMed: 26972063]
44. Choi SM, Liu H, Chaudhari P, Kim Y, Cheng L, Feng J, et al. Reprogramming of EBV-immortalized B-lymphocyte cell lines into induced pluripotent stem cells. Blood. 2011; 118:1801–1805. [PubMed: 21628406]
45. Rajesh D, Dickerson SJ, Yu J, Brown ME, Thomson JA, Seay NJ. Human lymphoblastoid B-cell lines reprogrammed to EBV-free induced pluripotent stem cells. Blood. 2011; 118:1797–1800. [PubMed: 21708888]
46. Mamdani F, Alda M, Grof P, Young LT, Rouleau G, Turecki G. Lithium response and genetic variation in the CREB family of genes. Am J Med Genet B. 2008; 147B:500–504.
47. Spitzer RL, Endicott J, Robins E. Research diagnostic criteria: rationale and reliability. Arch Gen Psychiatry. 1978; 35:773–782. [PubMed: 655775]
48. Endicott J, Spitzer RL. A diagnostic interview: the schedule for affective disorders and schizophrenia. Arch Gen Psychiatry. 1978; 35:837–844. [PubMed: 678037]
49. Lopez de Lara C, Jaitovich-Groisman I, Cruceanu C, Mamdani F, Lebel V, Yerko V, et al. Implication of synapse-related genes in bipolar disorder by linkage and gene expression analyses. Int J Neuropsychopharmacol. 2010; 13:1397–1410. [PubMed: 20667171]
50. Manchia M, Adli M, Akula N, Ardau R, Aubry JM, Backlund L, et al. Assessment of response to lithium maintenance treatment in bipolar disorder: a Consortium On Lithium Genetics (ConLiGen) Report. PLoS One. 2013; 8:e65636. [PubMed: 23840348]

51. Garnham J, Munro A, Slaney C, Macdougall M, Passmore M, Duffy A, et al. Prophylactic treatment response in bipolar disorder: results of a naturalistic observation study. J affect Disord. 2007; 104:185–190. [PubMed: 17442400]
52. Grof P, Cavazzoni P, Grof E, Garnham J, MacDougall M, O'Donovan C, Alda M. Is response to prophylactic lithium a familial trait? J Clin Psychiatry. 2002; 63:942–947. [PubMed: 12416605]
53. Okita K, Matsumura Y, Sato Y, Okada A, Morizane A, Okamoto S, et al. A more efficient method to generate integration-free human iPS cells. Nat Methods. 2011; 8:409–412. [PubMed: 21460823]
54. Rudy B. Diversity and ubiquity of K channels. Neuroscience. 1988; 25:729–749. [PubMed: 2457185]
55. Yu DX, Di Giorgio FP, Yao J, Marchetto MC, Brennand K, Wright R, et al. Modeling hippocampal neurogenesis using human pluripotent stem cells. Stem Cell Rep. 2014; 2:295–310.
56. Stern S, Segal M, Moses E. Involvement of potassium and cation channels in hippocampal abnormalities of embryonic Ts65Dn and Tc1 trisomic mice. EBioMedicine. 2015; 2:1048–1062. [PubMed: 26501103]
57. Jan LY, Jan YN. Voltage-gated and inwardly rectifying potassium channels. J Physiol. 1997; 505(Part 2):267–282. [PubMed: 9423171]
58. Erisir A, Lau D, Rudy B, Leonard CS. Function of specific K(+) channels in sustained high-frequency firing of fast-spiking neocortical interneurons. J Neurophysiol. 1999; 82:2476–2489. [PubMed: 10561420]
59. Connors BW, Gutnick MJ. Intrinsic firing patterns of diverse neocortical neurons. Trends Neurosci. 1990; 13:99–104. [PubMed: 1691879]
60. Martina M, Schultz JH, Ehmke H, Monyer H, Jonas P. Functional and molecular differences between voltage-gated K+ channels of fast-spiking inter-neurons and pyramidal neurons of rat hippocampus. J Neurosci. 1998; 18:8111–8125. [PubMed: 9763458]
61. Rudy B, Chow A, Lau D, Amarillo Y, Ozaita A, Saganich M, et al. Contributions of Kv3 channels to neuronal excitability. Ann NY Acad Sci. 1999; 868:304–343. [PubMed: 10414303]

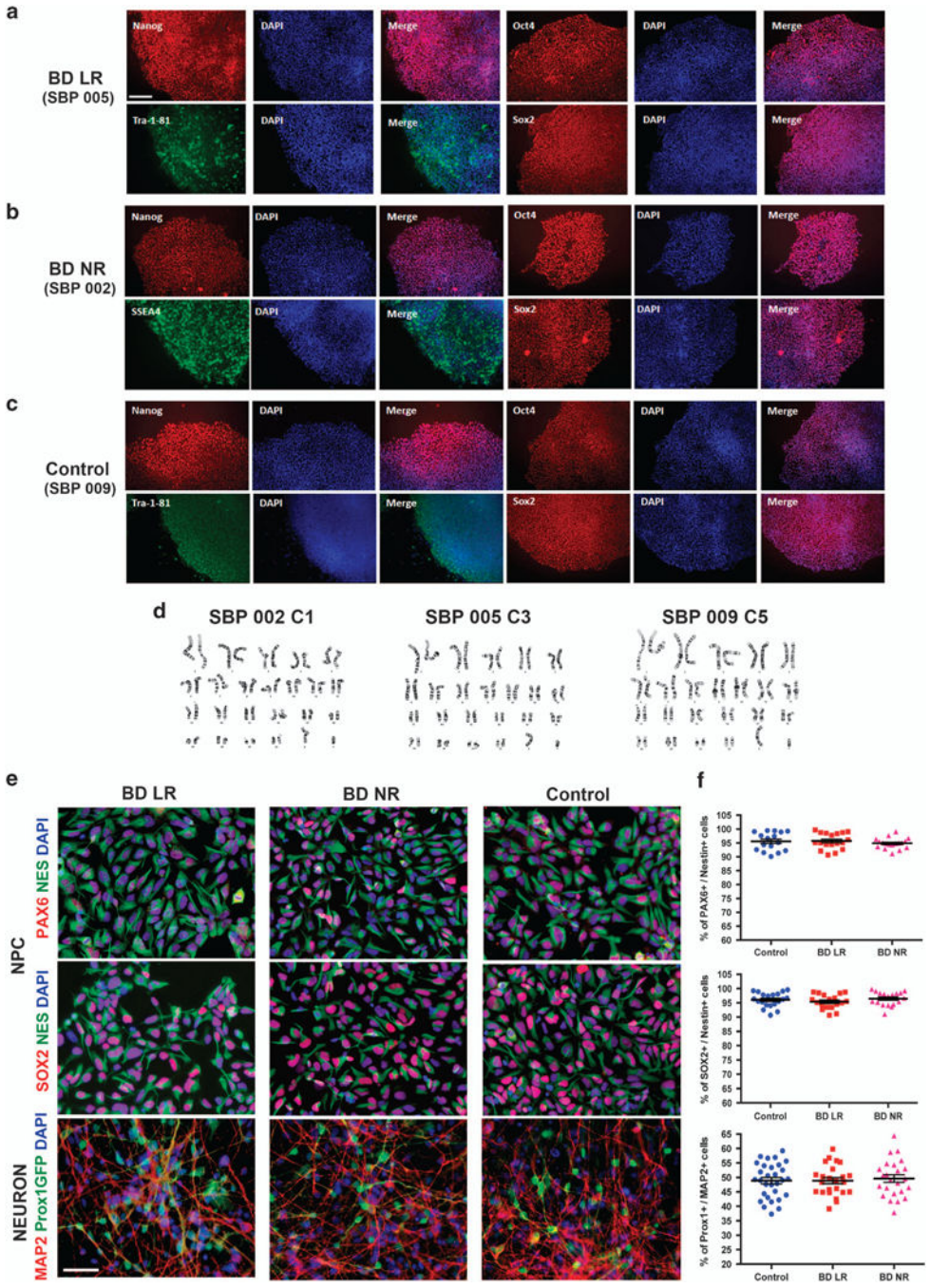

Figure 1.

Characterization of induced pluripotent stem cells (iPSCs) and neural cells derived from Epstein–Barr virus-immortalized B-lymphocytes from patients with bipolar disorder (BD). The figure shows representative examples of cells from BD patients who are lithium-responsive (LR), lithium-non-responsive (NR) and neurotypical controls. (**a–c**) Representative images of iPSC colonies showing expression of pluripotency markers (Nanog, Tra-1-81, Oct4 and Sox2); scale bar: 150 μm. (**d**) Representative examples of chromosome G-banding analysis of iPSC clones showing normal karyotype. (**e**)

Representative examples of neural progenitor cells (NPCs) expressing typical NPC markers Nestin, Pax6 and Sox2 and examples of neurons expressing the pan neuronal marker MAP2 and the hippocampus dentate gyrus (DG) granular cell marker Prox1. DG cells are evidenced by a vector expressing GFP under the control of a Prox1 promoter (Prox1::GFP); scale bar: 50 μm. (**f**) Graph plots showing the percentage of Pax6 or Sox2 over Nestin-positive cells and percentage of Prox1 over Map2-positive cells.

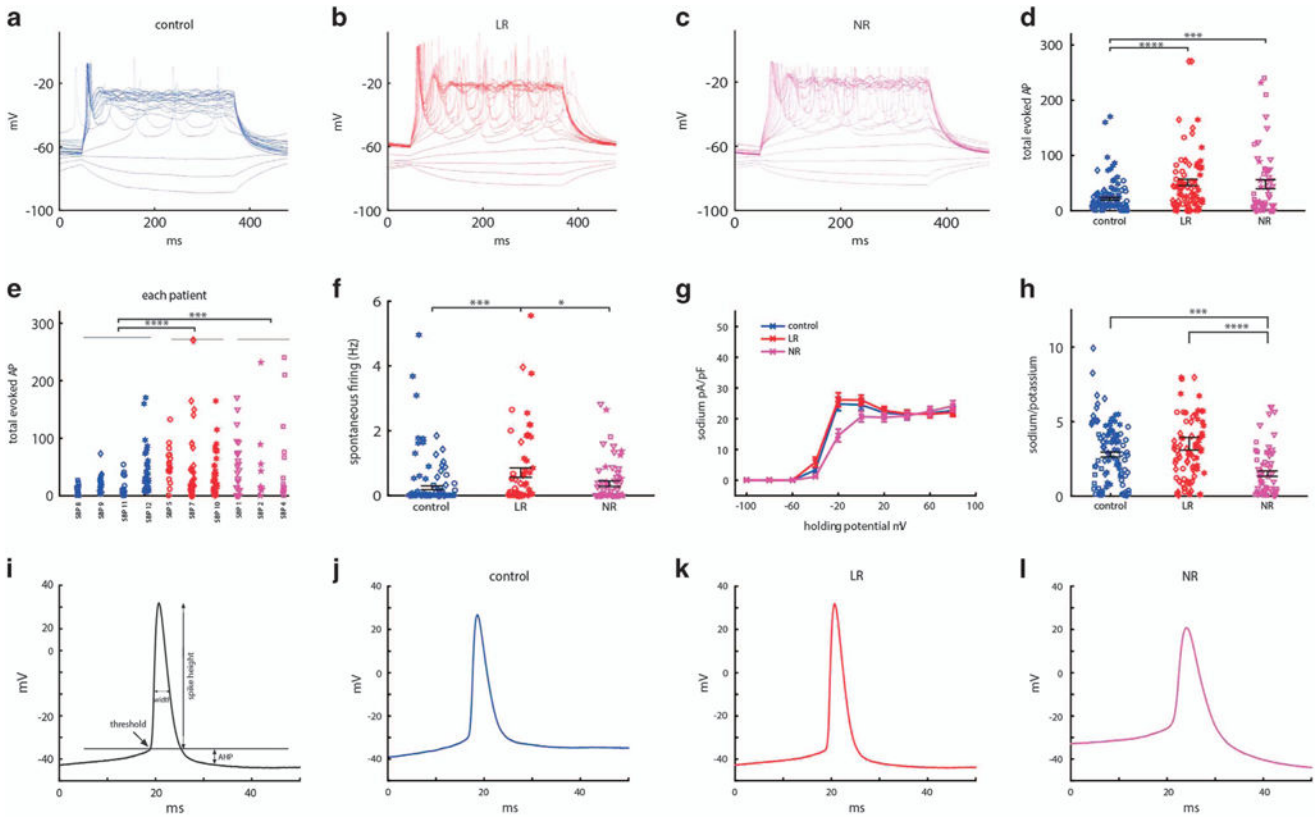

Figure 2.

Dentate gyrus granule-cell-like hippocampal neurons derived from patients with bipolar disorder (BD) are hyperexcitable at 3.5 weeks (20–30 days) postdifferentiation when comparing control patients' neurons (control $n = 95$ cells from four lines), lithium-responsive (LR) patients (LR $n = 84$ cells from three lines) and lithium-non-responsive (NR) patients (NR $n = 63$ cells from three lines), and spike shape is different between the three groups (control, LR and NR). (**a–c**) Representative recordings of evoked action potentials in current clamp mode of a (**a**) control (**b**) LR and (**c**) NR neuron. (**d**) Total number of evoked action potentials in 35 depolarization steps shows hyperexcitability of BD neurons. (**e**) Patient-by-patient plot of the total evoked action potentials. (**f**) Spontaneous action potential rate measured when the cell is typically held between −45 and −50 mV for 60 s. (**g**) Average of normalized sodium currents as a function of membrane holding potential display lower sodium current in NR neurons. (**h**) Average ratio of sodium current measured at −20 mV and slow potassium current measured at 20 mV display lower ratios of the currents in NR neurons. (**i**) Demonstration of action potential features. (**j–l**) Representative trace of an action potential of a control (**j**), LR (**k**) and NR neuron (**l**) displays a different spike shape between the three groups (see Supplementary Figure 1 for averages of the different features). LR neurons have a higher amplitude and narrower action potential compared with control neurons (**k**), whereas NR neurons have a lower amplitude and broader action potentials, with a more depolarized threshold for evoking an action potential (**l**). Identical symbols indicate cells from the same cell line. *$P<0.05$, **$P<0.01$. ***$P<0.001$ and ****$P<0.0001$.

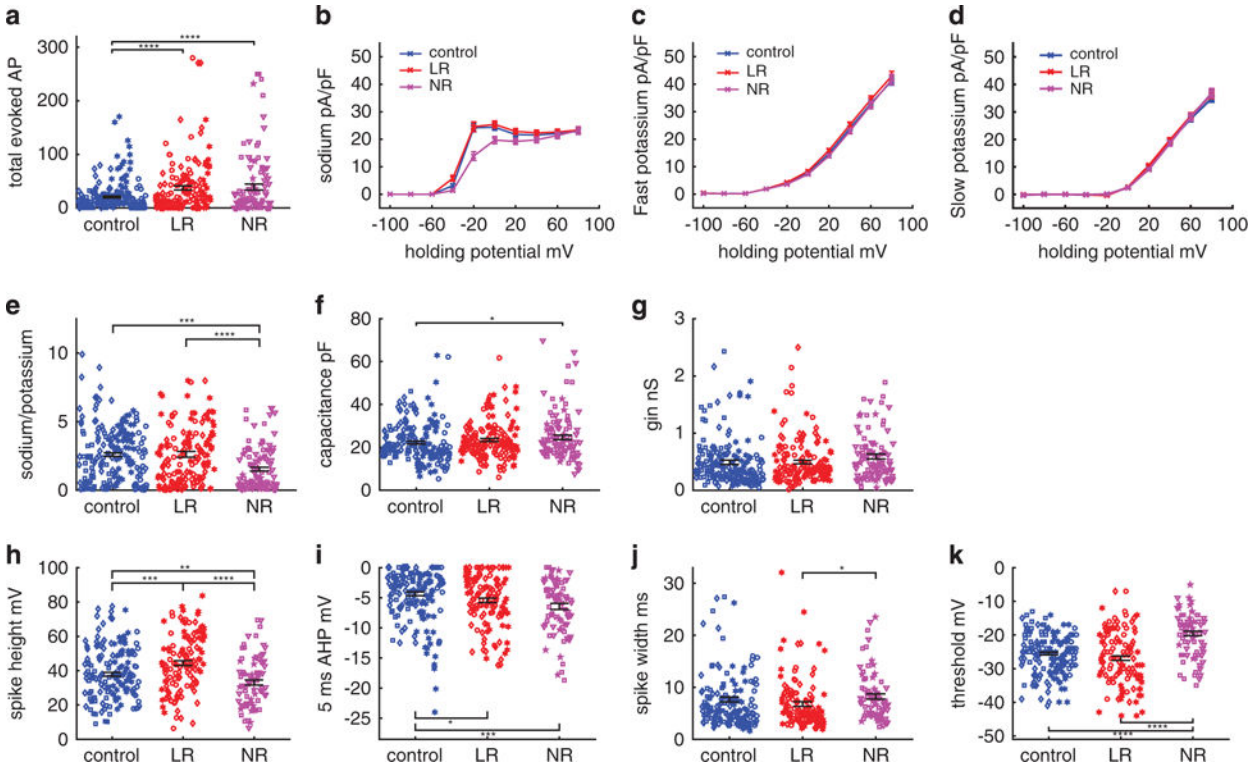

Figure 3.

Analysis of electrophysiological recordings from 10–45 days postdifferentiation reveals that the differences between the three groups (control, lithium-responsive (LR) and lithium-non-responsive (NR)) are maintained through the entire differentiation period and are enhanced when using this entire data set. Neurons are recorded over 10–45 days postdifferentiation (control $n = 195$ neurons from four lines, LR $n = 155$ neurons from three lines and NR $n = 112$ neurons from three lines). (**a**) Total number of evoked action potentials displays hyperexcitability in bipolar disorder neurons. (**b–e**) Averages of (**b**) sodium currents, (**c**) fast potassium currents, (**c**) slow potassium currents and (**e**) the ratio of sodium at − 20 mV to slow potassium currents at 20 mV. A reduction in the sodium currents and the sodium-to-potassium current ratio is observed for NR neurons. (**f**) Capacitance is increased in NR neurons. (**g**) Input conductance is similar in the three groups. (**h–k**) Characterization of spike shape. (**h**) Spike height is increased in LR neurons and decreased in NR neurons. (**i**) Five milliseconds after-hyperpolarization (AHP) amplitude is increased in LR neurons and even more in NR neurons. (**j**) Spike width is broader in NR compared with LR neurons. (**k**) The threshold for evoking an action potential is more depolarized in NR neurons. Identical symbols indicate cells from the same cell line. *P<0.05, **P<0.01, ***P<0.001 and ****P<0.0001.

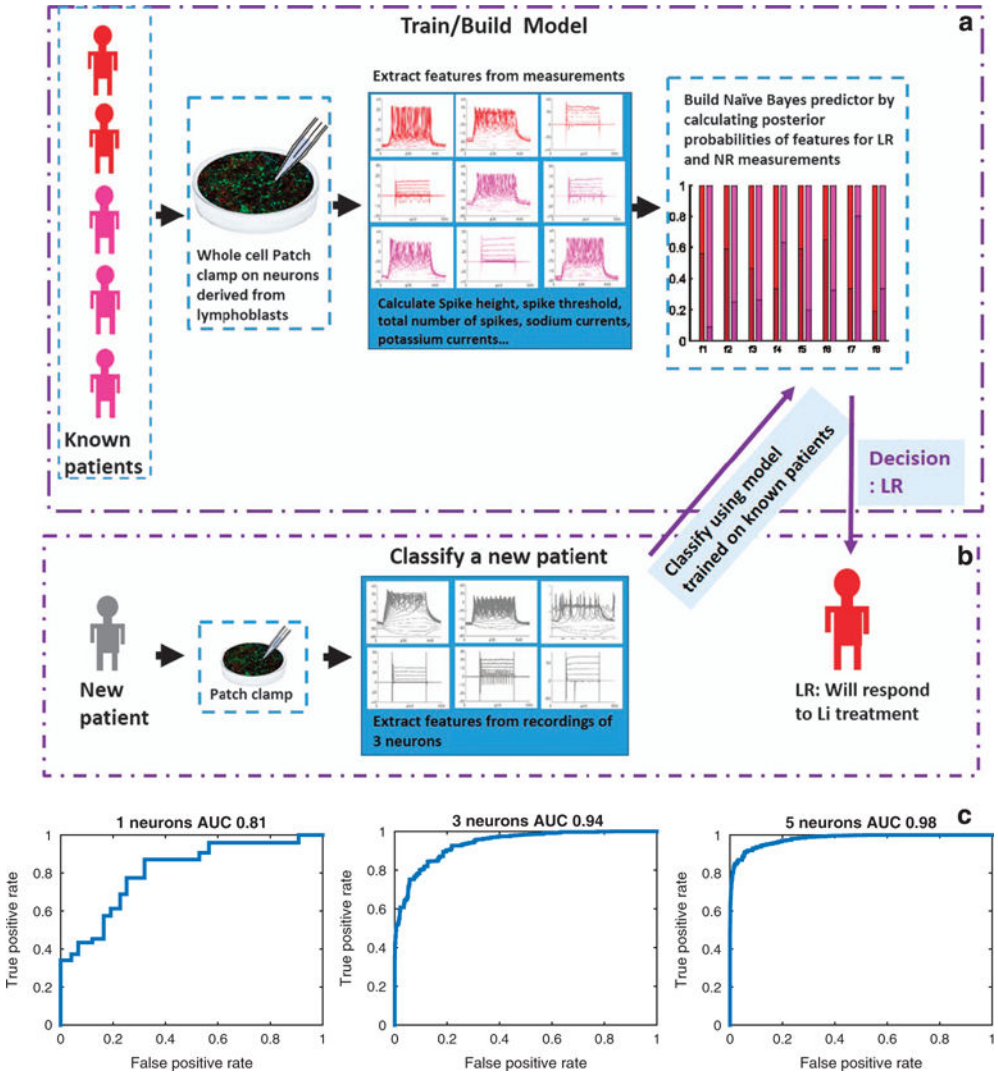

Figure 4.

Classification of a patient as responsive or non-responsive to lithium (Li) based on electrophysiological measurements. (**a**) Building the model: The model is trained on five of the six patients. Features such as spike height and spike threshold (see Materials and Methods for the entire list) are extracted from patch-clamp measurements and a Naïve Bayes (NB) model is built using posterior probabilities of the features that are calculated from the data set of the five patients. The model shown in the graph shows the posterior probabilities of each of the features when the patients are lithium (Li)-responsive (LR) patients (shades of red) and Li-non-responsive (NR) patients (shades of purple). (**b**) To classify a new patient, we use patch-clamp recordings from three cells. The NB model that was trained on measurements of the other patients is used to give a posterior score of the new patient as being NR or LR given the features extracted from its three-cell recordings. The decision is made based on the maximum posterior probability. (**c**) Performance is assessed pulling together classification of the six patients (each with a model trained on the other five patients) using a receiver-operating characteristics (ROC) curve and the area under the curve

(AUC). An ROC curve is shown for performance using one-cell recordings for classification, three-cell recordings or five-cell recordings. With five-cell recordings, the AUC is 0.98.

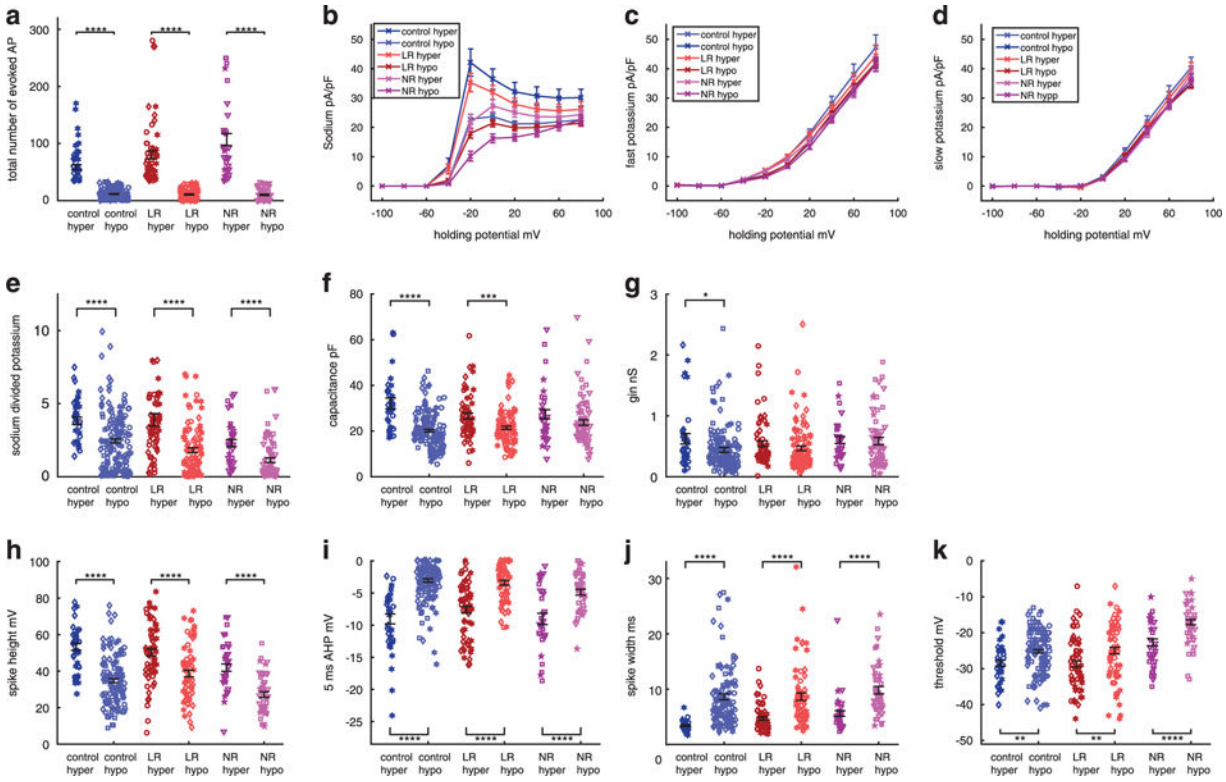

Figure 5.

Analysis of a subset of the data of the most excitable ‘hyper’ neurons (producing more than 35 evoked action potentials, see Materials and Methods) at 10–45 days postdifferentiation (control $n = 34$ neurons from four lines, lithium-responsive (LR) $n = 60$ neurons from three lines and lithium-non-responsive (NR) $n = 37$ neurons from three lines) vs the rest of the ‘hypo’ neurons. Each graph shows six groups with pair comparisons: ‘hyper’ control (dark blue) vs ‘hypo’ control (light blue), ‘hyper’ LR (dark red) vs ‘hypo’ LR (light red), and ‘hyper’ NR (dark purple) vs ‘hypo’ NR (light purple). Supplementary Figure 2 shows the comparisons between the other two subgroups. The first is a comparison between ‘hyper’ control vs ‘hyper’ LR and ‘hyper’ NR. The second is a comparison between the ‘hypo’ control vs ‘hypo’ LR and ‘hypo’ NR. (**a**) Total number of evoked action potentials is naturally increased in the ‘hyper’ groups. (**b–e**) Averages of (**b**) sodium currents, which are increased in the ‘hyper’ groups of control, LR and NR neurons, (**c**) fast potassium currents, which are increased in the ‘hyper’ groups of control, LR and NR neurons, (**d**) slow potassium currents (unchanged in ‘hyper’ vs ‘hypo’ neurons) and (**e**) the ratio of sodium at −20 mV to slow potassium currents at 20 mV, which is increased in the ‘hyper’ control, LR and NR neurons. (**f**) Capacitance is larger in the ‘hyper’ control and LR neurons. (**g**) Input conductance is larger in the ‘hyper’ control neurons. (**h–k**) Characterization of spike shape. (**h**) Spike height is increased in the ‘hyper’ control, LR and NR neurons. (**i**) Five milliseconds after-hyperpolarization (AHP) is larger in the ‘hyper’ control, LR and NR neurons. (**j**) Spike width is narrower in the ‘hyper’ control, LR and NR neurons. (**k**) Threshold for evoking an action potential is less depolarized in the ‘hyper’ control, LR and

NR neurons. Identical symbols indicate cells from the same cell line. *P<0.05, **P<0.01. ***P<0.001 and ****P<0.0001.

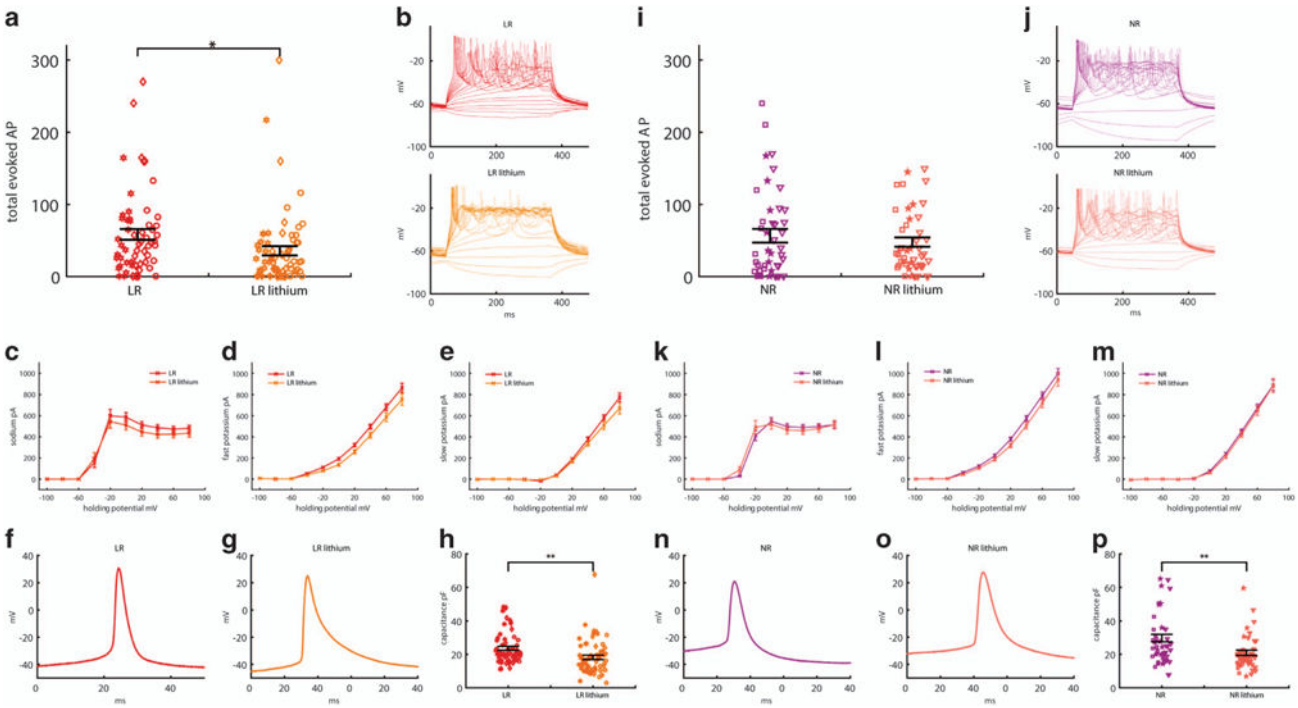

Figure 6.

Lithium (Li) decreases the excitability of neurons from Li-responsive (LR) patients ($n = 59$ neurons from three lines, and $n = 67$ Li-treated neurons from three lines) but not of neurons from lithium-non-responsive (NR) patients ($n = 44$ neurons from three lines, and $n = 47$ neurons from three lines treated with Li). Neurons patched at 22–30 days postdifferentiation. (**a–h**) Effects of Li on LR neurons. Red represents measurements without Li treatment; orange represents measurements with Li treatment. (**a**) Total number of evoked action potentials. (**b**) Representative recording of evoked action potentials in current clamp mode in LR (red) and Li-treated LR (orange) neurons (**c–e**) Averages of (**c**) sodium currents recorded in voltage clamp mode, decreased with Li treatment, (**d**) fast potassium currents, decreased with Li treatment and (**e**) slow potassium currents, unchanged after treatment. (**f** and **g**) A representative trace of an action potential shape of an untreated LR neuron (**f**) and a Li-treated LR neuron. (**g**) Li treatment causes broadening of the action potential and a reduction in the fast after-hyperpolarization (AHP) amplitude. See Supplementary Figure 3 for averages. (**h**) Capacitance decreased after Li treatment. (**i–p**) Similar analysis of the effect of Li on NR neurons (purple) and Li-treated NR neurons (pink) shows there is no significant decrease in neuronal excitability (**i** and **j**). (**k–m**) No significant differences in the sodium and slow potassium current were displayed. The fast potassium current decreased after treatment. (**n** and **o**) Li treatment caused a reduction in fast AHP amplitude and a shift towards a less depolarized threshold for evoking an action potential; see Supplementary Figure 3 for averages. (**p**) Similar to LR neurons, capacitance was reduced with Li treatment in NR neurons. Identical symbols indicate cells from the same cell line. *P<0.05 and **P<0.01.